UDC 666.26:66.017

*O.V. Savvova [a], T.V. Falko [a, b], O.V. Babich [a], Yu.O.Smyrnova [a], A.Yu. Melnykov [c]*

# STUDY OF THE INFLUENCE OF THE GLASS MELT REDOX STATE ON THE OPTICAL PROPERTIES OF CLEAR CONTAINER GLASS

**[a] O.M. Beketov Kharkiv National University of Urban Economy, Kharkiv, Ukraine**
**[b] Malinovsky Glassworks LLC, Malynivka urban village, Ukraine**
**[c] Scientific Research Institution «Ukrainian Scientific Research Institute of Ecological Problems», Kharkiv, Ukraine**

This paper investigates the mechanism of regulating the redox state of a soda-lime-silicate glass melt to produce clear container glass. It is demonstrated that the optical properties of the glass are determined by the $Fe^{2+}/Fe^{3+}$ ratio, which controls the absorption behavior in the UV–Vis–NIR range and the subsequent color formation of the material. It is established that reducing melting conditions promote an increase in the content of $Fe^{2+}/Fe_{tot}$ (up to 0.388) and $Fe^{2+}/Fe^{3+}\approx0.634$, leading to the appearance of a faint blue-green tint and a decrease in light transmittance. Conversely, weakly oxidizing conditions $Fe^{3+}/Fe_{tot}$ (up to 0.797) and $Fe^{2+}/Fe^{3+}\approx0.255$ ensure maximum transparency ($Tv\approx0.879$) and minimal coloration. It is shown that $Fe^{2+}$ governs the absorption in the near-infrared region, whereas $Fe^{3+}$ determines the absorption within the visible range of the spectrum. The obtained results confirm that managing the redox state by adjusting the batch composition, temperature, and oxygen fugacity is a key factor in ensuring the high optical quality of colorless pharmaceutical glass. The investigated glass samples are produced under industrial manufacturing conditions, which validates the practical feasibility of the proposed approaches.

**Keywords:** clear container glass, redox state, iron ions, optical properties, spectroscopy.

**DOI:** 10.32434/0321-4095-2026-168-5-40-49

***Introduction***

Clear glass and glass-ceramic materials are widely utilized across numerous fields of science and technology. In optics and photonics, they are employed for the fabrication of lenses, prisms, optical waveguides, and laser media due to their high optical homogeneity and tailored spectral characteristics [1]. In medicine, these materials serve as biocompatible systems that combine transparency with high mechanical strength [2]. In electronics, they function as substrates, protective coatings, and displays owing to their stable dielectric and optical properties, while in the energy sector, they are used as cover materials for solar panels and components of high-temperature systems due to the combination of transparency and chemical resistance [3]. In the construction industry, transparent and functionalized glasses are used for energy-efficient glazing systems with adjustable light and heat transmittance. In aerospace engineering, glasses and glass-ceramics are applied as thermal-shock-resistant optical elements capable of operating under extreme environmental conditions [4,5].

© O.V. Savvova, T.V. Falko, O.V. Babich, Yu.O.Smyrnova, A.Yu. Melnykov, 2026

This article is an open access article distributed under the terms and conditions of the Creative Commons Attribution (CC BY) license (https://creativecommons.org/licenses/by/4.0/).

In the pharmaceutical industry, the use of Type I borosilicate glass for the manufacturing of ampoules and vials is of paramount importance. Its high transparency ensures effective visual quality control of medicinal products, specifically for the detection of particulate matter, turbidity, and discoloration. Glass transparency is a key indicator of its commercial and technological quality, particularly for the colorless packaging of food products and beverages. The transparency of pharmaceutical glass containers (ampoules, vials, and cartridges) is not merely an aesthetic requirement but a critical functional parameter that ensures quality control, safety, and regulatory compliance. Transparent glass enables 100% visual identification of the solution for the presence of particulate matter, turbidity, discoloration, crystalline particles, and gas bubbles. The inability to perform visual inspection may result in particle contamination within parenteral preparations. Therefore, the evaluation of the optical characteristics of clear container glass is a mandatory requirement for determining its potential suitability as pharmaceutical-grade glassware according to pharmacopeias (such as USP <790> and European Pharmacopoeia 2.9.20) [6].

The optical characteristics of glass are determined by its base composition and the melting redox conditions, which establish the valence state of transition metals in the melt. Even trace concentrations of iron (0.02–0.1 wt.%) can significantly alter spectral transmittance in the visible and ultraviolet ranges due to the distinct absorption profiles of $Fe^{2+}$ and $Fe^{3+}$ ions [7]. Cerium-containing additives serve as an additional tool for controlling the redox state. The $Ce^{3+}/Ce^{4+}$ system acts as a redox buffer, stabilizing the $Fe^{2+}/Fe^{3+}$ ratio and enhancing the optical homogeneity of the glass. Studies have demonstrated that $Ce^{4+}$ can oxidize $Fe^{2+}$, thereby reducing the intensity of the green tint and increasing light transmittance in the visible range [8]. To compensate for the undesirable green tint, the industry traditionally utilizes manganese, which forms the $Mn^{2+}/Mn^{3+}$ redox couple. $Mn^{3+}$ ions exhibit absorption in the violet region, which optically neutralizes the coloration induced by $Fe^{2+}$ [9]. It was established that the efficiency of decolorization is directly dependent on the oxidizing melting conditions.

In the industrial production of glass containers, the redox state of the melt $Fe^{2+}/Fe^{3+}$ is controlled via the batch composition, the introduction of oxidizing/reducing agents, temperature, and the oxygen fugacity within the furnace. Oxygen fugacity ($fO_2$) is a thermodynamic parameter that characterizes the effective oxidizing capacity of the gaseous atmosphere and determines the ratio of valence states of multivalent elements within the glass melt [10].

An incorrect balance can lead to increased absorption in the visible region, an undesirable greenish or brownish tint, and reduced transparency of the products. Given contemporary requirements for colorless or weakly colored glass, particularly when utilizing recycled materials, the issue of redox state control becomes increasingly relevant. Therefore, investigating the redox potential in the production of clear pharmaceutical container glass will address critical applied challenges, enabling the manufacture of competitive products at domestic facilities.

It is known that for alkali-silicate glass, tetrahedral coordination is present for both $Fe^{2+}$ and $Fe^{3+}$ in the oxidized glass melt. The reduction process can alter the coordination number of iron from 4 to 6, depending on the oxidation state, glass composition, temperature, and local structure. It is clear that the iron content has a much stronger influence on the properties than the redox state. At lower temperatures, a distinct difference between reducing and oxidizing conditions is clearly observed, whereas at high temperatures, it remains within the measurement error. Changing the redox state has a significant effect on the transition temperature, density, microhardness, and CLTE. The trends in viscosity and structural changes depending on the $Fe^{2+}/Fe_{tot}$ and $Fe^{3+}/Fe_{tot}$ ratio confirm the consensus regarding the structural roles of $Fe^{3+}$ and $Fe^{2+}$:$Fe^{3+}$ ions have a stronger tendency toward network formation than $Fe^{2+}$ ions. Thus, the reduced iron ions in the structure play the role of both modifiers ($^{[6]}Fe^{2+}$ and $^{[6]}Fe^{3+}$) and network formers ($^{[4]}Fe^{2+}$ and $^{[4]}Fe^{3+}$).

Under open system conditions (contact with the atmosphere, $pO_2$=0.21 atm), the redox state of iron in glass is determined by the $Fe^{2+}/Fe^{3+}$, ratio, which directly affects the silicate network structure: $Fe^{2+}$ acts as a network modifier (depolymerization), while $Fe^{3+}$ acts as a network former (polymerization). With an increase in oxygen fugacity ($fO_2$), internal oxidation of the glass occurs, accompanied by a structural rearrangement.

It is known that $Fe^{3+}$ is characterized by intensive absorption in the short-wavelength region of the visible spectrum (yellow-brown tint), whereas $Fe^{2+}$ causes a broad absorption band in the near-IR region and forms a blue-green glass tint [11]. Light blue and dark blue tints in the glass coloration are caused by an increased concentration of [$Fe^{2+}$ $O_{6/2}$] structural groups. As the content of iron oxides increases, the integrated light transmittance of the glass naturally decreases to approximately 35%. Under oxidizing melting conditions, the glass coloration changes from blue-green to deep green tints (the $F^{2+}\overleftarrow{\rightarrow}F^{3+}$

equilibrium shifts to the right). The shift of the transmittance maximum toward the wavenumber region of approximately ~17,800 $cm^{-1}$ (560 nm) is associated with the predominance of [$Fe^{3+}$ $O_{4/2}$] structural groups.

The $Fe^{2+}$ /$Fe^{3+}$ ratio directly depends on the oxygen fugacity ($fO_2$). A decrease in $fO_2$ leads to an increase in the $Fe^{2+}$ fraction and a corresponding reduction in the transparency of clear glass containers, according to the law of mass action:

$$\left[\frac{Fe^{2+}}{Fe^{3+}}\right] \propto \left(fO_2\right)^{-1/4}.$$

Therefore, the higher the $fO_2$ value, the more $Fe^{3+}$ is present, resulting in the appearance of a yellow-brown glass tint. Conversely, the lower the $fO_2$ value, the more $Fe^{2+}$ is formed, the presence of which promotes a blue-green tint.

There is a correlation between the batch redox number, the $Fe^{2+}/Fe_{total}$ ratio, and the glass color [12].

Three independent kinetic regimes (modes) are distinguished, which can occur simultaneously but at different rates (Fig. 1) [12].

Mode I – molecular diffusion of $O_2$ (flux $jO_2$) is determined by the penetration of molecular oxygen. This process is unlikely for multicomponent silicates due to the low solubility of $O_2$.

Mode II – anionic diffusion of $O^{2-}$ (flux $jO^{2-}$) occurs at elevated temperatures. Under this regime, a high activation energy of $O^{2-}$ mobility is implemented.

Mode III – cationic diffusion (dominant) (flux $jM^{2+}$) is carried out by the diffusion of modifying cations. The regime that ensures the fastest advancement of the internal oxidation front dominates.

In most Fe-containing aluminosilicates ($T \geq 800^0C$, Fe~$10^{-2}$ at.%), mode III is implemented.

The main stages of the mode III process include:

1) diffusion of divalent cations ($M^{2+}$, particularly $Fe^{2+}$) to the surface;

2) reaction with atmospheric oxygen;

3) formation of surface crystalline oxides (spinels, simple oxides);

4) charge compensation through the flow of electron holes (h·).

Internal oxidation occurs not through the influx of oxygen, but due to the removal of cations, which leads to an increase in the $O^{2-}$/cation ratio.

Thus, the transparency of container glass is determined by a complex interaction between the chemical composition and the redox parameters of the melting process. Controlling the redox state by adjusting $fO_2$, temperature, and introducing redox additives serves as a key technological tool for ensuring the high light transmittance of colorless glass containers, especially when utilizing secondary raw materials with an increased iron content.

The aim of this work is to study the redox state of the glass melt in the technology of pharmaceutical container glass.

To achieve this aim, the following tasks were set:

– to investigate the redox state of iron in glass based on the $Fe^{2+}/Fe^{3+}$ ratio;

– to study the optical characteristics of glass containers;

– to evaluate the impact of the redox state of the glass melt in the technology of clear container glass.

***Experimental***

The experimental glass container samples were manufactured under industrial conditions at the Malinovsky Glassworks LLC in compliance with the current production technological regulations. To study the efficiency of decolorizing agents, a glass composition presented in Table 1 was selected.

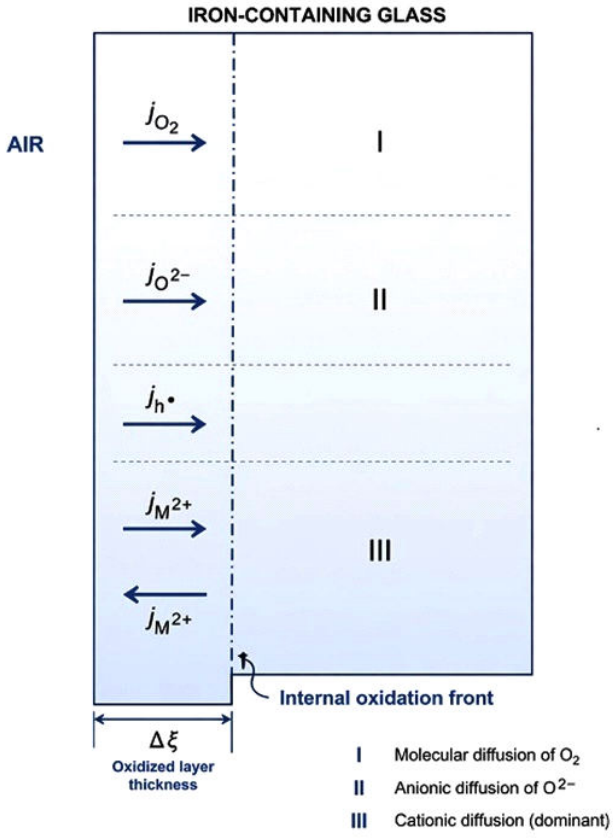



Fig. 1. Kinetic modes of oxidation by the external environment ($pO_2$=0.21 atm) of iron-rich aluminosilicate glass or melt [12]

The batch was formulated using quartz sand, limestone, soda ash, sodium sulfate, feldspar, and dolomite. The fraction of iron(II) oxide content in the batch for obtaining clear glasses is 0.0543 wt.% (quartz sand contains 0.0177 wt.%, limestone 0.0221 wt.%, soda ash 0.0021 wt.%, feldspar 0.012 wt.%, and dolomite 0.0004 wt. %).

To regulate the optical and color characteristics, cerium (IV) oxide, selenium, and cobalt oxide were introduced into the batch composition. The content of coal, introduced to create a reducing environment, was 300 g per 2500 kg of glass for glasses Nos. 1 and 2, 400 g for No. 3, and 200 g for No. 4.

The melting of the glass batch was carried out in a regenerative glass melting furnace of the HORN System "Deep End Melter" type, equipped with an air preheating system. The furnace design features a horseshoe-shaped flame flow configuration. The nominal capacity of the unit is 240 t/day, and the melting temperature range was maintained within 1484–1556$^0$C.

The total iron content ($Fe_{tot}$) in the raw materials and glasses was determined using Rigaku energy-dispersive X-ray fluorescence (EDXRF) spectrometers.

To determine the colorimetric characteristics of the glass samples, which had different thicknesses (the thickness of the samples No. 1, 2, 3 and 4 was 3.426 mm, 2.856 mm, 2.547 mm, and 3.721 mm, respectively), an PD-303 digital spectrophotometer (30303–10000 $cm^{-1}$) was used. Under standard light sources (C, A, D65), the color coordinates were determined in the CIELAB system (L*, a*, b*) (Fig. 2). The CIELAB system is a three-dimensional color model developed by the CIE in 1976, which is based on tristimulus color values. The L* parameter characterizes lightness (0 for black, 100 for white), a* corresponds to the red-green axis (negative values for green, positive values for red), and b* corresponds to the blue-yellow axis (negative values for blue, positive values for yellow). The a* and b* values range approximately from −128 to +128.

The analysis of color characteristics was also performed in the CIE XYZ coordinates (Fig. 3) using a chromaticity diagram (Maxwell's triangle), where the spectral locus covers the range of 30303–10000 $cm^{-1}$. The dominant wavelength (DWL) was determined as a parameter characterizing the color position on the spectral scale and related to its optical properties. The white point corresponds to the standard illuminant D65. The processing of experimental data was carried out using Chromaд software, which provides spectroscopic analysis (transmittance, reflectance, absorption) and calculation of colorimetric parameters of valence state ($Fe^{3+}$ and $Fe^{2+}$) [2].

The glass structure was investigated using FTIR spectroscopy on a Shimadzu IR Affinity-1S Fourier transform spectrometer (wavenumber range of 7800–400 $cm^{-1}$) and UV–Vis–NIR spectroscopy, covering the ultraviolet, visible, and partially near-infrared spectral regions, on a KFK-3 spectrometer (wavenumber range of 32000–11000 $cm^{-1}$).

***Results and discussion***

According to the energy-dispersive X-ray fluorescence (EDXRF) analysis results, the $Fe_{tot}$ content for the glass samples was determined to be 0.06 wt.%. The investigated glass samples (Nos. 1–4) are colorless and are characterized by a high level of light transmittance (Tv≈0.873–0.879) in the range of 30303–10000 $cm^{-1}$, which indicates low optical absorption (Table 2). The CIE xy color coordinates are close to the neutral point of white light, and the high values of lightness L* (94.69–95.11) confirm the high transparency of the material. The a* and b* parameters are near zero, indicating the absence of pronounced chromatic tints, although a slight increase in the yellow component is observed in sample No. 4. In practice, different tints of transparent glass, which are determined by manufacturers and product

Table 1

**Chemical composition of experimental glass, refining and decolorizing components**

| Component | Content | | |
|---|---|---|---|
| Base composition of experimental glass, wt.% | | | |
| $SiO_2$ | 72.4 | | |
| $Al_2O_3$ | 2.2 | | |
| CaO+MgO | 11.9 | | |
| $Na_2O+K_2O$ | 13.5 | | |
| Refining and decolorizing agents per 2500 kg of glass, g (wt.%) | | | |
| coal | 200 (0.008) | 300 (0.012) | 400 (0.016) |
| selenium | 30 (0.0012) | | |
| cobalt oxide | 3.5 (0.00014) | | |
| cerium(IV) oxide | 250 (0.01) | | |
| sodium sulfate | 18300 (0.732) | | |

demand, are defined by specific L*, a*, and b* values and are unique to each brand.

It was established that the optical characteristics of the glass correlate with the redox state of iron. For sample No. 4, which exhibits the highest $Fe^{3+}/Fe_{tot}$ fraction (up to 0.797), a slight shift toward increased yellowness (b*) and a change in the dominant wavelength are observed, whereas the highest $Fe^{2+}/Fe_{tot}$ ratio (up to 0.388) for sample No. 3 contributes to a negligible decrease in the green color characteristics. The color rendering index Ra for all samples is very high (99.4–99.5), which indicates virtually perfect color reproduction. Thus, the investigated glasses are characterized by high optical quality, and minor differences in color parameters are caused by changes in the $Fe^{2+}/Fe^{3+}$ ratio within the glass structure.

To obtain colorless glass, it is necessary to minimize the fraction of $Fe^{2+}$ without shifting into an excessively oxidizing region, so as not to impair refining and melting stability, while ensuring the following values of the $Fe^{2+}/Fe^{3+}$ ratio and the contents of $Fe^{2+}$ and $Fe^{3}z$ :$Fe^{2+}/Fe^{3+}$=0.20–0.35, the $Fe^{2+}$ fraction ≈15–25% of total Fe, and the $Fe^{3+}$ fraction ≈75–85% of total Fe. Analysis of the colorimetric and spectrophotometric characteristics of the experimental colorless glass samples with various coal contents showed a clear dependence of the optical parameters on the redox state of iron (Table 2).

The analysis of the redox state of the experimental samples of colorless container glass showed a significant variation in the $Fe^{2+}/Fe^{3+}$ ratio within the range of 0.255–0.635. It was established that samples Nos. 1–3 are characterized by an increased content of divalent iron (0.316–0.388), which corresponds to reducing melting conditions due to the introduction of 0.0012–0.0016 wt.% of coal and promotes the formation of a blue-green tint of glass as a result of intensive $Fe^{2+}$ absorption in the red and near-infrared regions spectral regions. This is confirmed by more negative values of the a* coordinate (up to −0.44) and a slight decrease in light transmittance (Tv=0.8734–0.8787).

By contrast, sample No. 4, characterized by a carbon content of 0.008 wt.%, exhibits a regular decrease in the $Fe^{2+}/Fe^{3+}$ ratio to 0.255, with an $Fe^{2+}/Fe_{tot}$ fraction of 0.203. This corresponds to mildly oxidizing melting conditions, which are optimal for the production of clear container glass. Under such conditions, the contribution of $Fe^{2+}$ to coloration is minimized, the $Fe^{3+}/Fe_{tot}$ fraction increases (0.797), the green color component is reduced, and the maximum light transmittance (Tv=0.8789) is achieved. The obtained results are consistent with modern concepts regarding the effect of the iron valence state

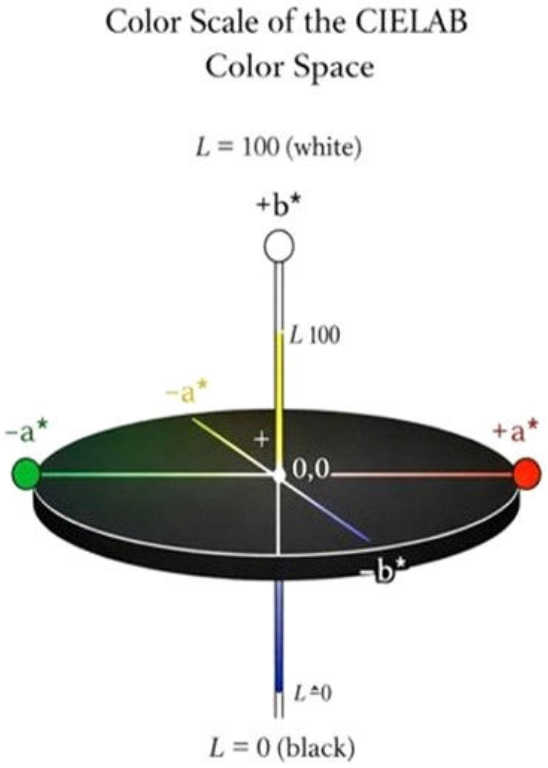



Fig. 2. CIELAB color scale

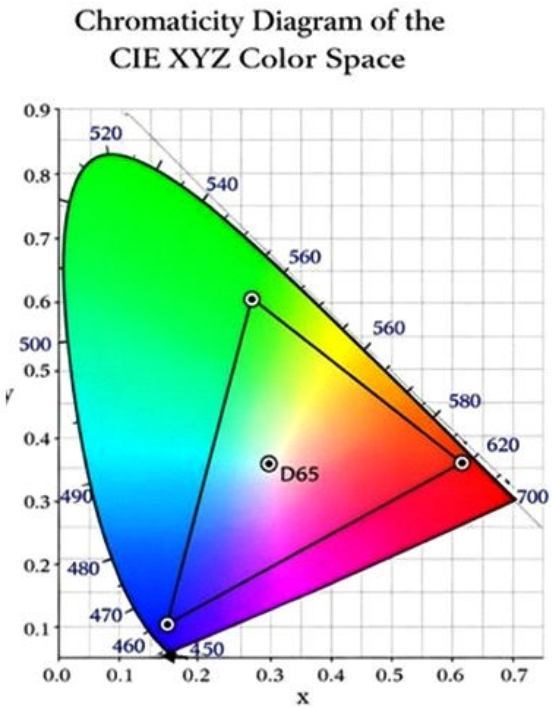



Fig. 3. CIE XYZ color space chromaticity diagram (Maxwell's triangle)

on the optical properties of silicate glasses and confirm the necessity of maintaining the $Fe^{2+}/Fe^{3+}$ ratio within the range of 0.20–0.35 to ensure the high optical quality of clear container glass.

Determining the coordination state of $Fe^{2+}$ and $Fe^{3+}$ in glass is essential for establishing its structural role, the redox state of the system, and its impact on the optical and physicochemical properties of the material. Let us consider the change in the coordination state of glass-forming and modifying components, including iron, for the investigated glass sample No. 4.

The FTIR spectrum of the investigated glass (7800 $cm^{-1}$–400 $cm^{-1}$) exhibits a structure typical for silicate systems, dominated by the vibrational modes of the Si–O–Si framework (Fig. 4). The intense band in the range of ≈1000–1100 $cm^{-1}$ is associated with the asymmetric stretching vibrations of Si–O–Si, whereas the band at ≈800 $cm^{-1}$ corresponds to the symmetric stretching vibrations of the silicate network. The low-frequency region (≈600–500 $cm^{-1}$) reflects bending vibrations and the contribution of modifying cations, including iron ions, which can affect the local coordination of $SiO_4$ tetrahedra.

The presence of $Al_2O_3$ in the investigated glass materials promotes the formation of a three-dimensional network involving [$AlO_4$] groups and [$SiO_4$] tetrahedra. The presence of Si–O–Al bonds in the glass is evidenced by an absorption band in the 720–780 $cm^{-1}$ region. The absence of vibrations in the 580–680 $cm^{-1}$ region, which are characteristic of [$AlO_6$] octahedra, also indicates that aluminum exists in a four-coordinated state 710–780 $cm^{-1}$, isomorphously substituting silicon to form a mixed aluminosilicate network. In the glass structure, magnesium ions in four-coordination enter the silicate framework as [$MgO_4$] tetrahedra and are present as Si–O–Mg structural fragments, as evidenced by the bands with a maximum in the 550–700 $cm^{-1}$ region (Fig. 4).

In the high-frequency region of the FTIR spectrum, a weak absorption band is observed with a maximum near 5400–5500 $cm^{-1}$, corresponding to the combination vibrations of hydroxyl groups and molecular water. The presence of this band indicates a minor content of OH-groups or adsorbed moisture in the glass.

In FTIR spectra, $Fe^{2+}$–O vibrations are typically observed in the 400–600 $cm^{-1}$ region; however, they are weak and strongly overlap with the bending vibration bands of the silicate framework. The absence of distinct absorption bands in the 550–700 $cm^{-1}$

Table 2

**Color, light transmittance, and iron redox state indicators for samples with different thicknesses**

| Indicators | Marking of experimental glass samples | | | |
|---|---|---|---|---|
| | No. 1 | No. 2 | No. 3 | No. 4 |
| Thickness, mm | 3.426 | 2.856 | 2.547 | 3.721 |
| Minimum wavelength, $cm^{-1}$ | 30303 | 30303 | 30303 | 30303 |
| Maximum wavelength, $cm^{-1}$ | 10000 | 10000 | 10000 | 10000 |
| Color | colorless | colorless | colorless | colorless |
| CIE XYZ–X | 86.1 | 85.6 | 85.4 | 84.9 |
| CIE XYZ–Y | 87.9 | 87.5 | 87.3 | 86.9 |
| CIE XYZ–Z | 102.7 | 102.4 | 102.2 | 100.9 |
| CIE xy–x | 0.3112 | 0.3106 | 0.3106 | 0.3114 |
| CIE xy–y | 0.3176 | 0.3176 | 0.3177 | 0.3185 |
| Dominant wavelength (DWL), $cm^{-1}$ | 17420 | 17686 | 17689 | 17531 |
| Saturation (S) | 0.006 | 0.005 | 0.005 | 0.010 |
| CIELab–L* | 95.11 | 94.95 | 94.88 | 94.69 |
| CIELab–a* | –0.15 | –0.42 | –0.44 | –0.46 |
| CIELab–b* | 0.68 | 0.59 | 0.61 | 1.05 |
| CIELab–Cab | 0.69 | 0.72 | 0.75 | 1.15 |
| CIELab–hab | 102.2 | 125.3 | 125.7 | 113.4 |
| $Fe^{2+}/Fe^{3+}$ | 0.4970 | 0.4619 | 0.6339 | 0.2547 |
| $Fe^{2+}/Fe_{tot}$ | 0.332 | 0.316 | 0.388 | 0.203 |
| $Fe^{3+}/Fe_{tot}$ | 0.668 | 0.684 | 0.612 | 0.797 |
| Tv (light transmittance) | 0.8787 | 0.8749 | 0.8734 | 0.8789 |
| Ra (Color Rendering Index) | 99.5 | 99.4 | 99.4 | 99.5 |

range may indicate the predominant occurrence of $Fe^{3+}$ in tetrahedral [$FeO_4$] coordination (450–570 $cm^{-1}$), which participates in the formation of the glass framework [13].

The main spectral features are associated with structural changes in the silicate units (800–1300 $cm^{-1}$) and the vibrations of Fe–O bonds in octahedral and tetrahedral positions (≈380 and 570 $cm^{-1}$) [13].

In the glass compositions under consideration, the coordination state of $Fe^{3+}$ is determined by the molar ratio of $(Na_2O+CaO):(Al_2O_3+Fe_2O_3)>1$, where $Na_2O$ and CaO act as oxygen-donor oxides. In the presence of an excess of $(R_2O+RO)$, both iron and aluminum ions form tetrahedral oxygen complexes such as $(Fe^{3+}O_{4/2})^-Na^+$ and $(Fe^{3+}O_{4/2})^{2-}Ca^{2+}$. Thus, for the investigated glass with a ratio of $(Na_2O+CaO):(Al_2O_3+Fe_2O_3)>1$, a predominantly tetrahedral coordination of $Fe^{3+}$ is characteristic. At high concentrations and under reducing conditions, which are not typical for the investigated glass, a significant portion of iron can exist as $Fe^{3+}$ ions in octahedral coordination, as well as $Fe^{2+}$ ions in both octahedral and tetrahedral coordination.

However, due to the overlapping of bands with the vibrations of the aluminosilicate framework, a definitive conclusion regarding the coordination state of iron based solely on FTIR spectroscopy data remains insufficiently substantiated.

The transmission and absorption spectra of the transparent glass under study in the UV–Vis–NIR range are characterized by high light transmittance, indicating a low content of coloring impurities, primarily iron compounds. It is known that in silicate glasses, iron can exist in the form of $Fe^{2+}$ and $Fe^{3+}$ ions, which form characteristic absorption bands in the near-infrared, visible, and ultraviolet regions of the spectrum. Nevertheless, for the glass under study, the intensity of these bands is negligible, pointing to a low concentration of iron and its minimal effect on the optical properties of the material (Fig. 5). The absence of intense absorption near 5000 $cm^{-1}$ indicates a negligible content of divalent iron [14].

In the visible spectral region, no distinct absorption bands characteristic of $Fe^{3+}$ (20000–26000 $cm^{-1}$) [15] are observed, which is consistent with the high transparency of the glass and the absence of noticeable coloration. This indicates a very low concentration of trivalent iron or its presence in quantities insufficient to significantly affect the optical characteristics of the material.

Thus, the optical properties of the investigated glass are predominantly determined by the intrinsic transparency of the aluminosilicate matrix, whereas the contribution of iron ions to the formation of the absorption spectrum is minimal. The high transparency of the glass confirms both the low content of coloring impurities and the homogeneity of the formed glass

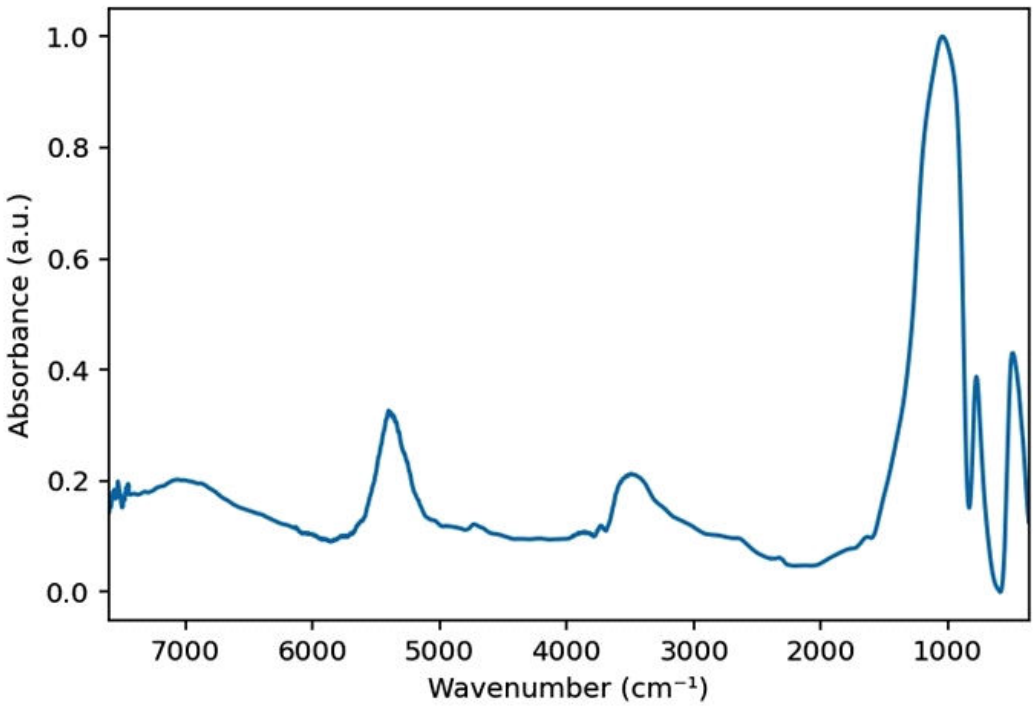



Fig. 4. FTIR spectrum of the investigated glass

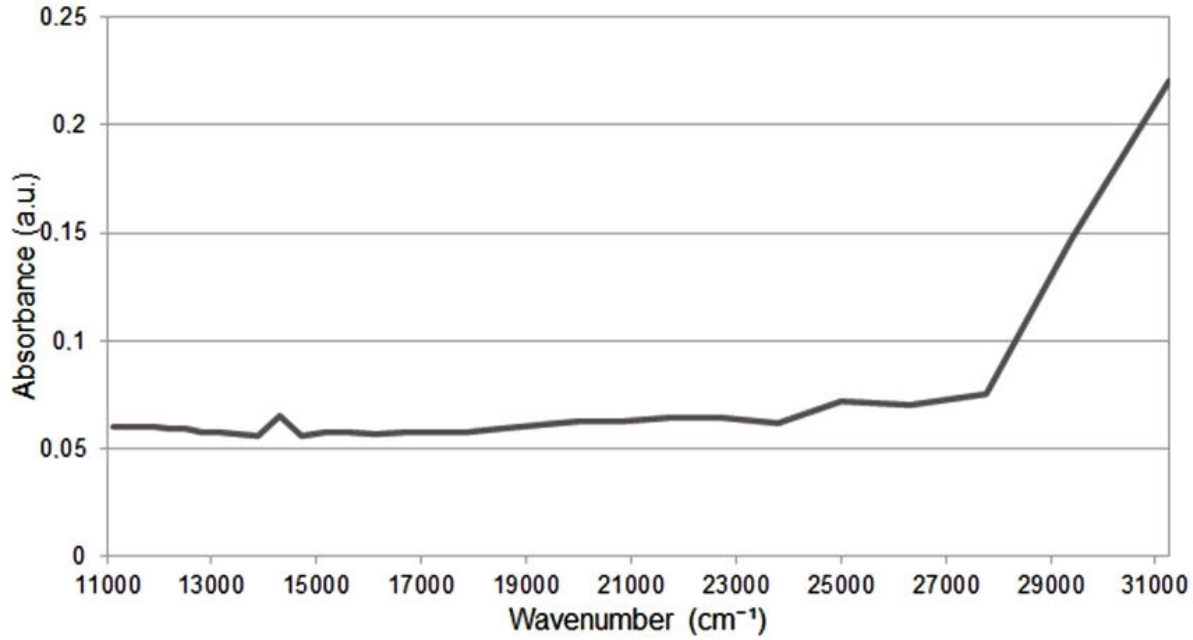



Fig. 5. UV–Vis–NIR spectrum of the investigated glass

structure.

***Conclusions***

Under the industrial conditions of Malinovsky Glassworks LLC, the composition of soda-lime-silicate glass was optimized for the production of clear glass containers. The investigated glass samples are characterized by high light transmittance and nearly neutral color parameters, indicating their superior optical quality. Minor variations in coloration are driven by shifts in the $Fe^{2+}/Fe^{3+}$ ratio, which affects the position and intensity of the chromatic characteristics of the glass. It was established that the redox state of the glass melt is the determining factor in the formation of the optical properties of clear container glass and directly controls the $Fe^{2+}/Fe^{3+}$ ratio within the silicate network structure. It was found that the optimal optical performance of colorless glass (maximum light transmittance (Tv≈0.879) and minimal coloration) is achieved at an $Fe^{2+}/Fe^{3+}$ ratio of approximately 0.255 ($Fe^{3+}/Fe_{tot}$=0.797). This corresponds to weakly oxidizing melting conditions with the following content of refining and decolorizing agents (wt.%): carbon 0.008, selenium 0.0012, CoO 0.00014, $CeO_2$ 0.01, and $Na_2SO_4$ 0.732.

It was confirmed that the investigated glass is characterized by high transparency in the UV–Vis–NIR range, indicating a low content of coloring impurities, particularly iron compounds. In the near-infrared spectral region, weak absorption bands are observed, which can be associated with trace amounts of $Fe^{2+}$ ions and vibrational transitions of hydroxyl groups. In the visible region, the intense absorption characteristic of $Fe^{3+}$ is practically absent, which is consistent with the colorlessness and high light transmittance of the glass.

According to the IR spectroscopy results, the formation of a highly polymerized aluminosilicate structure, composed predominantly of [$SiO_4$] and [$AlO_4$] tetrahedra, was established. The presence of absorption bands characteristic of Si–O–Al bonds confirms the formation of a three-dimensional aluminosilicate framework, whereas the absence of bands inherent to octahedrally coordinated aluminum indicates its incorporation into the glass matrix in tetrahedral coordination. The obtained results confirm that the optical properties of the investigated material are primarily determined by the intrinsic transparency of the aluminosilicate matrix and the high homogeneity of the formed structure.

It was proven that effective control of the redox state by adjusting the oxygen fugacity, batch composition, and the introduction of redox additives serves as a key technological tool for producing high-quality colorless container glass.

## REFERENCES

1. *Patra P., Annapurna K.* Transparent tellurite glass-ceramics for photonics applications: a comprehensive review on crystalline phases and crystallization mechanisms // Prog. Mater. Sci. – 2022. – Vol.125. – Art. No. 100890.

2. *Development* of calcium phosphate-silicate glass ceramic materials resistant to biochemical and mechanical destruction / Savvova O.V., Shimon V.M., Babich O.V., Fesenko O.I. // Funct. Mater. – 2020. – Vol.27. – No. 4. – P.767-773.

3 *Moor D., Rosenberg V., Vasiliev M.* High-transparency clear glass windows with large PV energy outputs // Glass Conf. Proc. – 2022. – Vol.8. – P.1-8.

4. *Effect* of the structure of lithium-silicate glasses on the mechanical properties of transparent glass-ceramic materials / Savvova O.V., Topchyi V.L., Babich O.V., Belyakov R.O. // Strength Mater. – 2018. – Vol.50. – P.874-879.

5. *Investigation* of structure formation in lithium silicate glasses on initial stages of nucleation / Savvova O.V., Babich O.V., Kuriakin M., Grivtsova A., Topchyi V.L. // Funct. Mater. – 2017. – Vol.24. – No. 2. – P.311-317.

6. *European* Directorate for the Quality of Medicines & HealthCare (EDQM). European Pharmacopoeia, General Chapter 2.9.20. Particulate Contamination: Visible Particles. – Strasbourg: Council of Europe, European Pharmacopoeia, 11th Edition. – 2025.

7. *Фалько Т.В., Саввова О.В., Бабіч О.В.* Дослідження ефективності застосування знебарвлюючих агентів у промисловому виробництві безбарвного тарного скла // Вісн. НТУ «ХПІ». Сер. хімія, хім. технол. та екол. – 2025. – № 2(14). – С.78-85.

8. *The effect* of decolorizing agent on the optical properties of high iron contents soda-lime silicate glass / Meechoowas E., Petchareanmongko B., Jampeerung P., Tapasa K. // Key Eng. Mater. – 2017. – Vol.766. – P.28-33.

9. *Identification* and methods of influencing the oxidation states of Mn and Ce in silicate glasses / Volf J., Varak P., Buryi M., Kormunda M., Nekvindova P. // Materials. – 2025. – Vol.18. – No. 9. – Art. No. 1948.

10. *Saleem M.H., Ali S., Ali S.* An innovative approach towards decolorization of tint and enhancing the optical & physical properties of high iron $Na_2O–CaO–SiO_2$ glass by co-doping with $Ce^{4+}/Nd^{3+}$ // Opt. Mater. – 2024. – Vol.157. – Art. No. 116160.

11. *The ancient* glass decoloration technology based on the Fe–Mn redox pairs revived to improve the chemical stability of $Fe_2O_3$-containing borosilicate glass for medical application / Fu J., Zhang H., Shi S., Liu S. // Ceram. Int. – 2024. – Vol.50. – No. 22. – P.46673-46682.

12. *Neuville D.R., Cormier L.* Redox variations in glass manufacturing: effects of oxygen fugacity and temperature on glass and melt properties // Mater. Lett. – 2025. – Vol.382. – Art. No. 137821.

13. *Development* of iron–silicate composites by waste glass and iron or steel powders / Rada R., Vermesan H., Rada S., Leostean C., Manea D.L., Culea E. // Molecules. – 2023. – Vol.28. – Art. No. 6296.

14. *Carl R., Gerlach S., Russel C.* The effect of composition on UV–Vis–NIR spectra of iron-doped glasses in the systems $Na_2O/MgO/SiO_2$ and $Na_2O/MgO/Al_2O_3/SiO_2$ // J. Non-Cryst. Solids. – 2007. – Vol.353. – No. 3. – P.244-249.

15. *Volotinen T.T., Parker J.M., Bingham P.A.* Concentrations and site partitioning of $Fe^{2+}$ and $Fe^{3+}$ ions in a soda–lime–silica glass obtained by optical absorbance spectroscopy // Phys. Chem. Glass. Eur. J. Glass Sci. Technol. B. – 2008. – Vol.49. – No. 5. – P.258-270.

Received 15.06.2026
Revised 03.09.2026
Accepted 10.09.2026
Published 28.10.2026

## ДОСЛІДЖЕННЯ ВПЛИВУ ОКИСНО-ВІДНОВНОГО СТАНУ СКЛЯНОГО РОЗПЛАВУ НА ОПТИЧНІ ХАРАКТЕРИСТИКИ ПРОЗОРОГО ТАРНОГО СКЛА

***Саввова О.В., Фалько Т.В., Бабіч О.В., Смирнова Ю.О., Мельников А.Ю.***

У статті досліджено механізм регулювання окисно-відновного стану натрій-кальцій-силікатного скляного розплаву для отримання прозорого тарного скла. Показано, що оптичні властивості скла визначаються співвідношенням $Fe^{2+}/Fe^{3+}$, яке контролює характер поглинання в UV–Vis–NIR діапазоні та формування кольору матеріалу. Встановлено, що відновні умови плавлення сприяють підвищенню вмісту $Fe^{2+}/Fe_{tot}$ (до 0,388) та $Fe^{2+}/Fe^{3+}\approx0,634$, що приводить до появи слабкого синьо-зеленого відтінку та зниження світлопропускання, тоді як слабоокиснювальні умови $Fe^{3+}/Fe_{tot}$ (до 0,797) та $Fe^{2+}/Fe^{3+}\approx0,255$ забезпечують максимальну прозорість (Tv≈0,879) і мінімальне забарвлення. Показано, що $Fe^{2+}$ визначає поглинання у ближній ІЧ-області, а $Fe^{3+}$ – у видимому діапазоні спектра. Отримані результати підтверджують, що керування редокс-станом шляхом регулювання складу шихти, температури та кисневої фугитивності є ключовим чинником забезпечення високої оптичної якості безбарвного фармацевтичного скла. Досліджувані зразки скла одержано в умовах промислового виробництва, що підтверджує практичну реалізованість запропонованих підходів.

**Ключові слова:** прозоре тарне скло, редокс-стан, іони заліза, оптичні властивості, спектроскопія.

**STUDY OF THE INFLUENCE OF THE GLASS MELT REDOX STATE ON THE OPTICAL PROPERTIES OF CLEAR CONTAINER GLASS**

***O.V. Savvova [a], T.V. Falko [a, b], O.V. Babich [a, *], Yu.O.Smyrnova [a], A.Yu. Melnykov [c]***

**[a] O.M. Beketov Kharkiv National University of Urban Economy, Kharkiv, Ukraine**

**[b] Malinovsky Glassworks LLC, Malynivka urban village, Ukraine**

**[c] Scientific Research Institution «Ukrainian Scientific Research Institute of Ecological Problems», Kharkiv, Ukraine**

**[*] e-mail: lenysjababich@gmail.com**

This paper investigates the mechanism of regulating the redox state of a soda-lime-silicate glass melt to produce clear container glass. It is demonstrated that the optical properties of the glass are determined by the $Fe^{2+}/Fe^{3+}$ ratio, which controls the absorption behavior in the UV–Vis–NIR range and the subsequent color formation of the material. It is established that reducing melting conditions promote an increase in the content of $Fe^{2+}/Fe_{tot}$ (up to 0.388) and $Fe^{2+}/Fe^{3+}\approx0.634$, leading to the appearance of a faint blue-green tint and a decrease in light transmittance. Conversely, weakly oxidizing conditions $Fe^{3+}/Fe_{tot}$ (up to 0.797) and $Fe^{2+}/Fe^{3+}\approx0.255$ ensure maximum transparency (Tv≈0.879) and minimal coloration. It is shown that $Fe^{2+}$ governs the absorption in the near-infrared region, whereas $Fe^{3+}$ determines the absorption within the visible range of the spectrum. The obtained results confirm that managing the redox state by adjusting the batch composition, temperature, and oxygen fugacity is a key factor in ensuring the high optical quality of colorless pharmaceutical glass. The investigated glass samples are produced under industrial manufacturing conditions, which validates the practical feasibility of the proposed approaches.

**Keywords:** clear container glass; redox state; iron ions; optical properties; spectroscopy.

**REFERENCES**

1. Patra P, Annapurna K. Transparent tellurite glass-ceramics for photonics applications: a comprehensive review on crystalline phases and crystallization mechanisms. *Prog Mater Sci.* 2022; 125: 100890. doi: 10.1016/j.pmatsci.2021.100890.

2. Savvova OV, Shimon VM, Babich OV, Fesenko OI. Development of calcium phosphate-silicate glass ceramic materials resistant to biochemical and mechanical destruction. *Funct Mater.* 2020; 27(4): 767-773. doi: 10.15407/FM27.04.767.

3. Moor D, Rosenberg V, Vasiliev M. High-transparency clear glass windows with large PV energy outputs. *Challenging Glass Conf Proc.* 2022; 8: 1-8. doi: 10.47982/cgc.8.404.

4. Savvova OV, Topchyi VL, Babich OV, Belyakov RO. Effect of the structure of lithium-silicate glasses on the mechanical properties of transparent glass-ceramic materials. *Strength Mater.* 2018; 50: 874-879. doi: 10.1007/s11223-019-00034-3.

5. Savvova O, Babich O, Kuriakin M, Grivtsova A, Topchyi V. Investigation of structure formation in lithium silicate glasses on initial stages of nucleation. *Funct Mater.* 2017; 24(2): 311-317. doi: 10.15407/fm24.02.311.

6. European Directorate for the Quality of Medicines & HealthCare (EDQM). European Pharmacopoeia, General Chapter 2.9.20. Particulate Contamination: Visible Particles. Strasbourg: Council of Europe, European Pharmacopoeia, 11th Edition, 2025.

7. Falko TV, Savvova OV, Babich OV. Doslidzhennia efektyvnosti zastosuvannia znebarvliuiuchykh ahentiv u promyslovomu vyrobnytstvi bezbarvnoho tarnoho skla [Research into the effectiveness of using decolorizing agents in the industrial production of colorless container glass]. *Visnyk NTU «KhPI». Seriia: Khimiia, Khimichna Tekhnolohiia ta Ekolohiia.* 2025; 2(14): 78-85. (*in Ukrainian*). doi: 10.20998/2079-0821.2025.02.12.

8. Meechoowas E, Petchareanmongko B, Jampeerung P, Tapasa K. The effect of decolorizing agent on the optical properties of high iron contents soda-lime silicate glass. *Key Eng Mater.* 2017; 766: 28-33. doi: 10.4028/www.scientific.net/KEM.766.28.

9. Volf J, Varak P, Buryi M, Kormunda M, Nekvindova P. Identification and methods of influencing the oxidation states of Mn and Ce in silicate glasses. *Materials.* 2025; 18(9): 1948. doi: 10.3390/ma18091948.

10. Saleem MH, Ali S, Ali S. An innovative approach towards decolorization of tint and enhancing the optical and physical properties of high iron $Na_2O–CaO–SiO_2$ glass by co-doping with $Ce^{4+}/Nd^{3+}$. *Opt Mater.* 2024; 157: 116160. doi: 10.1016/j.optmat.2024.116160.

11. Fu J, Zhang H, Shi S, Liu S. The ancient glass decoloration technology based on the Fe–Mn redox pairs revived to improve the chemical stability of $Fe_2O_3$-containing borosilicate glass for medical application. *Ceram Int.* 2024; 50(22): 46673-46682. doi: 10.1016/j.ceramint.2024.09.019.

12. Neuville DR, Cormier L. Redox variations in glass manufacturing: effects of oxygen fugacity and temperature on glass and melt properties. *Mater Lett.* 2025; 382: 137821. doi: 10.1016/j.matlet.2024.137821.

13. Rada R, Vermesan H, Rada S, Leostean C, Manea DL, Culea E. Development of iron–silicate composites by waste glass and iron or steel powders. *Molecules.* 2023; 28: 6296. doi: 10.3390/molecules28176296.

14. Carl R, Gerlach S, Russel C. The effect of composition on UV–Vis–NIR spectra of iron-doped glasses in the systems $Na_2O/MgO/SiO_2$ and $Na_2O/MgO/Al_2O_3/SiO_2$. *J Non-Cryst Solids.* 2007; 353(3): 244-249. doi: 10.1016/j.jnoncrysol.2006.11.010.

15. Volotinen TT, Parker JM, Bingham PA. Concentrations and site partitioning of $Fe^{2+}$ and $Fe^{3+}$ ions in a soda–lime–silica glass obtained by optical absorbance spectroscopy. *Phys Chem Glass Eur J Glass Sci Technol B.* 2008; 49(5): 258-270.